

One can compensate the cable delay during data analysis. Since the frequency span for a BTF measurement is much smaller than the 3 dB frequency bandwidth of feedback system, S_{21} parameter and $B(\omega)$ is only different by a proportionality constant. One can just do a linear fit to determine the proportional constant, which is given by the following:

$$\frac{eI_b(\omega)S_{\perp}K_{\perp}D}{-i\gamma m_0 c Q_0 \Omega_0}$$

The above arguments will not hold if the frequency span of the BTF measurement is beyond the 3 dB bandwidth of feedback system. To improve the signal to noise ratio, a time domain gating technique[5] is applied to the analysis. Because we are interested in the low frequency range of the transverse impedance, a detector optimized for low frequency signals was built as depicted in Figure 2.

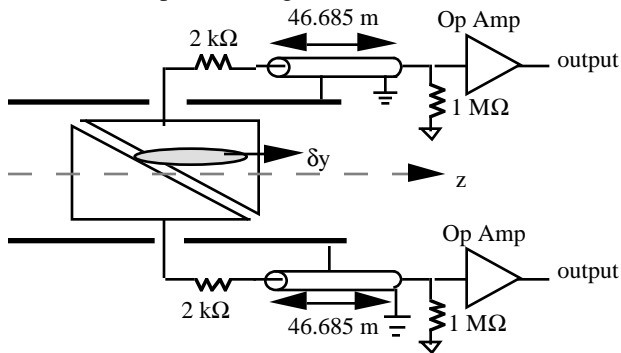


Figure 2: The configuration of beam position monitor used for BTF measurements.

II. RESULTS OF BEAM EXPERIMENTS

Vertical BTF measurements were done at the injection energy of the MR, 8 GeV, with debunched beam. Figure 4 and 5 are examples of measured raw data. Figure 6 is the stability diagram after the time domain gating technique is applied. The signal is still quite noisy. The fitting results are shown as dashed lines in Figures 6 -9. Only the central portion of resonance response is used for fitting because of the noise. The fitting result for vertical impedance is shown in Figure 10.

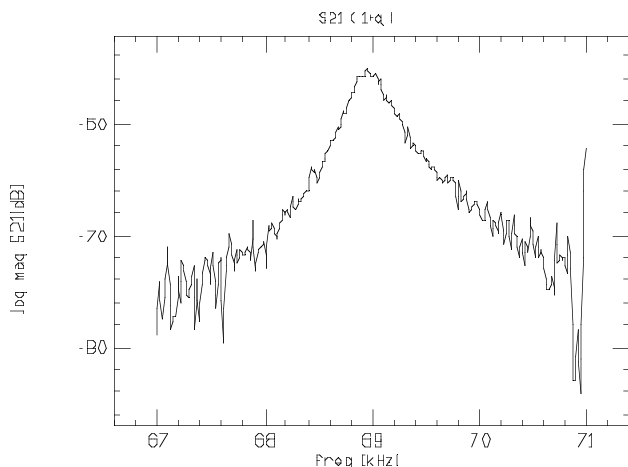


Figure 3: Amplitude of S21(raw data) for the n=1+q sideband.

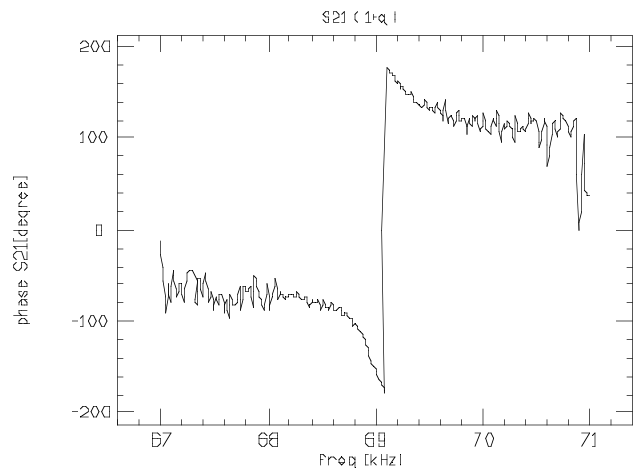


Figure 4: Phase of S21 (raw data) for the n=1+q sideband.

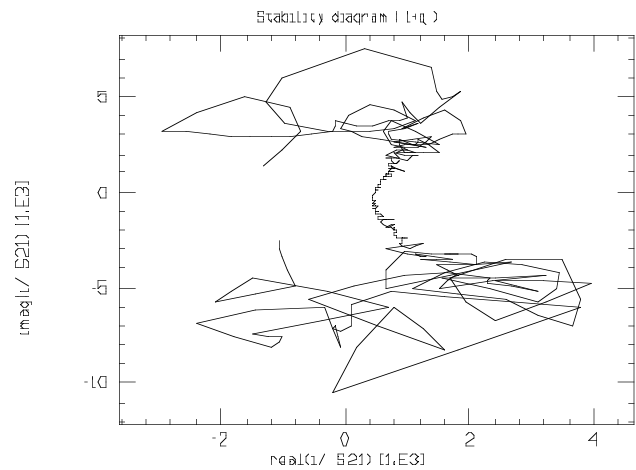


Figure 5: Stability diagram for the n=1+q betatron sideband processed by applying the time domain gating technique.

The revolution frequency of Main Ring is 47.4 kHz and the fractional tune is 0.4. The beam pipe is made of stainless steel and the thickness is 0.065". If we assume only beam pipe of circular cross section is used around the accelerator, we can calculate the vertical impedance. The result is depicted in Figure 11.

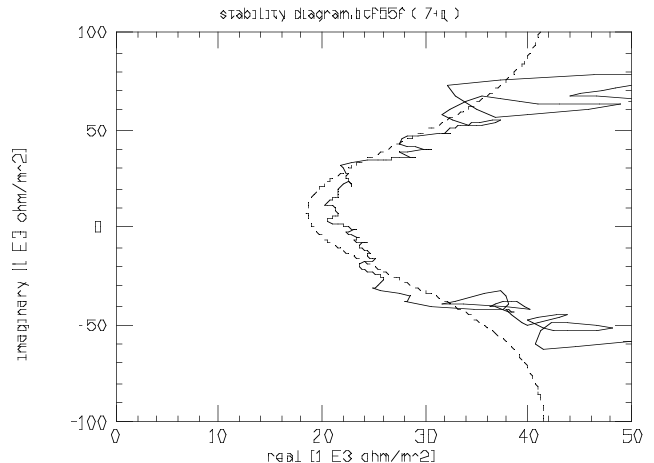


Figure 6: Stability diagram for the n=7+q betatron sideband.

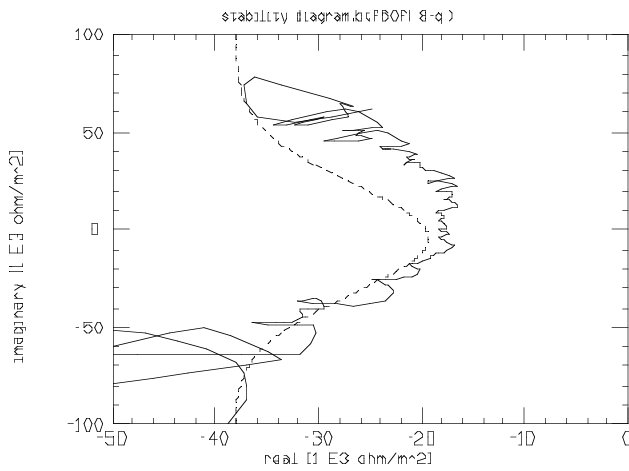


Figure 7: Stability diagram for the $n=8-q$ betatron sideband.

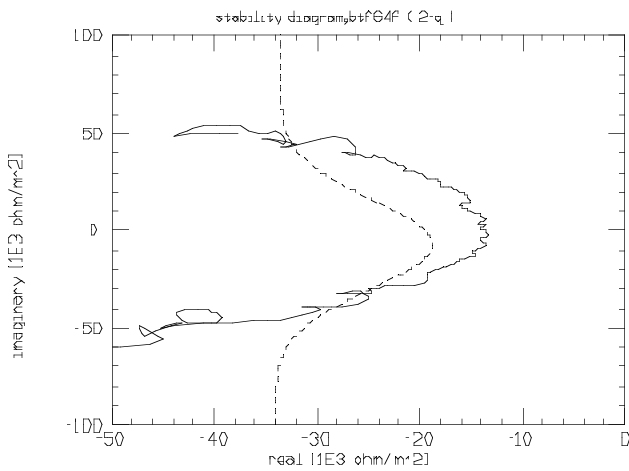


Figure 8: Stability diagram for the $n=2-q$ betatron sideband.

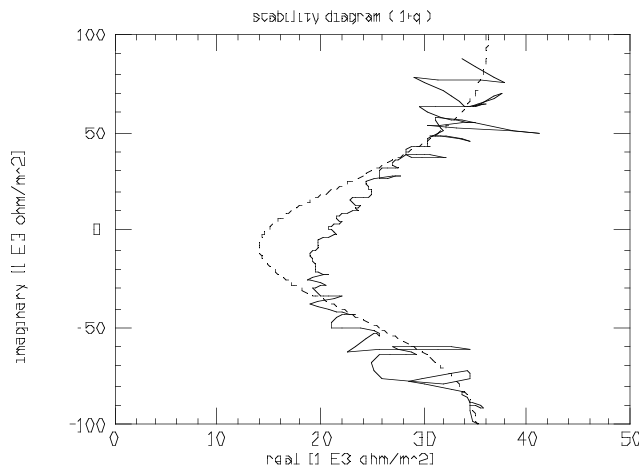


Figure 9: Stability diagram for the $n=1+q$ betatron sideband.

We are particularly interested in the vertical impedance of the first few betatron sidebands because of evidence showing the signs of collective beam instabilities due to the resistive wall impedance[6]. The results from BTF measurements do not show the characteristic $\omega^{-1/2}$ dependence of resistive wall impedance. Other sources besides wall resistance of the beam

pipe may contribute to the observed phenomena. Work is still underway to improve the accuracy of measurements.

III. ACKNOWLEDGEMENT

The authors would like to thank U. Oeftiger for many helpful discussions.

IV. REFERENCES

- [1] A. Hofmann, B. Zotter, IEEE Transactions NS-24, No.3 (1977)1487.
- [2] M. Chanel, U. Oeftiger, CERN/PS 93-44(AR).
- [3] D. Boussard, CERN SPS/86-11(ARF).
- [4] M. Month, M. Dienes(eds.), AIP Conference Proceedings , No.249, p.537, American Institute of Physics, 1992.
- [5] U. Oeftiger, F. Caspers, CERN/PS/AR/Note 92-19.
- [6] G. Jackson, IEEE Particle Accelerator Conference, vol.3, (1991)1755.

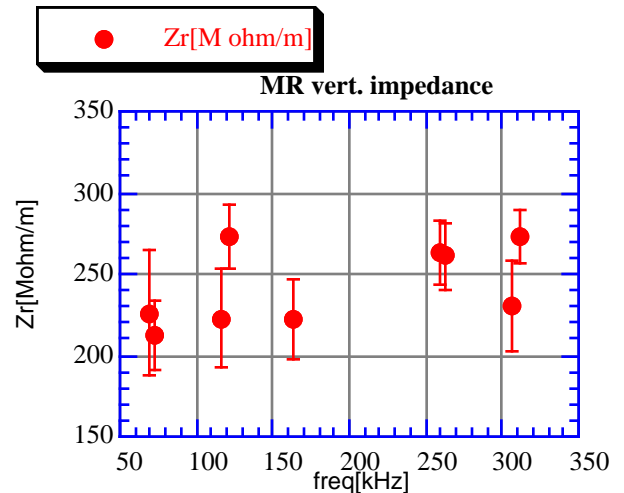


Figure 10: The vertical impedance of the Fermilab Main Ring from BTF measurements. The unit of y axis is in $M\Omega/m$.

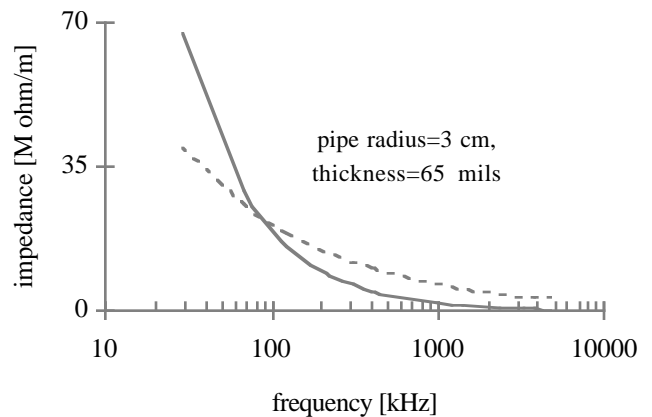


Figure 11: Theoretical calculation of vertical impedance for Main Ring. Only the real part is plotted. The dashed line is the value for thick wall model and the solid line is the thin wall model.